A membrane model for spatiotemporal coupling

Research Report
ISSN 0167-9708
Coden: TEUEDE

Eindhoven
University of Technology
Netherlands

Faculty of Electrical Engineering

A Membrane Model for Spatiotemporal Coupling

by
A.C. den Brinker

EUT Report 90-E-241
ISBN 90-6144-241-9

June 1990

Eindhoven University of Technology Research Reports

EINDHOVEN UNIVERSITY OF TECHNOLOGY

Faculty of Electrical Engineering
Eindhoven The Netherlands

ISSN 0167- 9708

Coden: TEUEDE

A MEMBRANE MODEL FOR SPATIOTEMPORAL COUPLING

by

A.C. den Brinker

EUT Report 90-E-241
ISBN 90-6144-241-9

Eindhoven
June 1990

CIP-GEGEVENS KONINKLIJKE BIBLIOTHEEK, DEN HAAG

Brinker, A.C. den

A membrane model for spatiotemporal coupling / by A.C. den
Brinker. - Eindhoven: Eindhoven University of Technology,
Faculty of Electrical Engineering. - Fig. - (EUT report,
ISSN 0167-9708; 90-E-241)
Met lit. opg., reg.
ISBN 90-6144-241-9
SISO 599.7 UDC 612.84.001.57 NUGI 822
Trefw.: visuele systemen; modellen.

Abstract

A model is proposed for spatiotemporal coupling within the transient visual system. The main features of the model are linearity, rotation symmetry and parsimonious use of parameters. The spatial transfer function of the model has a low-pass character with a cut-off frequency that depends on the temporal frequency. For the transient system the model can be completely parametrized using subthreshold measurements of impulse responses. The model is in agreement with physiological data on lateral information spread within the retina. The model was tested for predictions on flashed and sinusoidal stimuli and agrees in all major aspects with the experimental data.

Brinker, A.C. den
A MEMBRANE MODEL FOR SPATIOTEMPORAL COUPLING.
Faculty of Electrical Engineering, Eindhoven University of Technology,
Eindhoven, The Netherlands, 1990.
EUT Report 90-E-241

Author's address:
Dr.ir. A.C. den Brinker
Electrical Circuits and Systems Group
Faculty of Electrical Engineering
Eindhoven University of Technology
P.O. Box 513
NL-5600 MB Eindhoven
The Netherlands

Contents

1 Introduction

Much research on visual processing is focussed on the threshold behaviour of the visual system. By threshold behaviour is meant the magnitude of physical variables of the stimulus in order to be on the brink of being seen or not seen.

The importance of this kind of research is partly due to its applicability to technical realizations of visual information displays. Knowledge of the threshold behaviour can give criteria for the design of visual equipment. Two kinds of boundaries can be stated: one for the information that should be seen, the other for visual artifacts of the equipment that are allowable.

In order to use the experimental data on threshold behaviour for the above-mentioned purpose, a convenient way to represent these data is provided by a model which is adequate and yet as simple as possible. Unfortunately, the behaviour of the visual system of even small signals around some steady background level (as is usually the case for threshold experiments) is far from simple, or rather, is not well understood.

The processing of visual stimuli at threshold level is usually assumed to be performed in different pathways that are operating in parallel. In the temporal domain there are usually two channels operating in parallel postulated (Kulikowski and Tolhurst, 1973; Roufs, 1974a; Breitmeyer and Ganz, 1976). These two channels are called the *sustained* and the *transient* channel, based on an electrophysiological concept (Cleland *et al.*, 1971). In some psychophysical studies (e.g., Mandler and Makous, 1984) three temporal channels are advocated.

There is not only a difference in temporal characteristics of the different channels, but also in spatial features. In the spatial domain the number of different channels ranges from four (Wilson and Bergen, 1979) to (virtually) infinity (Koenderink and Van Doorn, 1978). It is generally accepted that a channel which is most sensitive to high-temporal frequencies is spatially low-tuned and vice versa (Breitmeyer and Ganz, 1976; Legge, 1978).

The *transient* system is tuned to high temporal and to low spatial frequencies (e.g., Legge, 1978). Associated with the transient system is the percept of agitation (Roufs, 1974a). The different channels are assumed to be spatiotemporally coupled. This can be seen from the de Lange curves, where the threshold amplitude of a (gated) sinusoid is plotted versus its (temporal) frequency. For larger field sizes de Lange curves are obtained, which show higher cut-off and peak frequencies (Roufs and Bouma, 1980; see also Section 8). Since the transient system is most sensitive to large stimuli we expect to find the most pronounced spatiotemporal interaction in this channel. Furthermore, there is much experimental material available to model this channel (Roufs and Blommaert, 1981; Roufs and Bouma, 1980). For these reasons we have concentrated our research on spatiotemporal coupling on the transient system.

From physiological experiments there is also evidence of spatiotemporal coupling. Detwiler *et al.* (1978, 1980) found an information spread in the retina of the turtle that becomes faster for larger field sizes. This is similar to the psychophysical findings of the variation in the de Lange curves as shown in Roufs and Bouma (1980) and Section 8.

Many models have been proposed on either spatial or temporal behaviour. However, many phenomena cannot be accounted for in just a spatial or a temporal model, and spatiotemporal ones are scarce (Korn and von Seelen, 1972; Marko, 1981). In this article a spatiotemporal model is proposed, and it is argued that this model can account for several phenomena associated with the transient channel. Also a quantitative comparison of the model behaviour and experimental data is made in this article. Since the point of view that is taken in deriving a description for spatiotemporal interaction is fairly general, it is hoped that the model is also applicable to data outside of those discussed here.

The spatiotemporal model derived here is *not* derived from physiological data on the behaviour of single neurons. The reason for this is that, firstly, we do not know what would be the relevant data for this modelling, and secondly, that we want to model psychophysical behaviour, i.e. responses of a mass of neurons. How to relate single neuron activity to the activity of a mass of neurons would, in our view, involve too many assumptions. Instead, we start from a general partial differential equation, a kind of relation between input and output signals that is often used in physics to describe the behaviour of a thin medium. This kind of modelling is essentially a black-box approach to account for the behaviour of a layer of neurons (such as are found in the retina). How this may be realized is not relevant for the modelling of psychophysical data. Nevertheless, we will consider an electrical network that can be described by the partial differential equation (PDE). In this way, a possible realization is shown and the parameters of the PDE are interpreted as physically realizable impedances.

A large number of restrictions is imposed on the PDE. One of these is linearity. Although the visual system as a whole does not act as a linear system (even at threshold level), there are indications that at least within a single channel linearity is applicable (de Lange, 1952; Roufs, 1974a; Krauskopf, 1980; Roufs and Blommaert, 1981; Blommaert and Roufs, 1987). From the PDE a transfer function is derived, and the root locus diagrams of these transfer functions are discussed. It is shown that the model can be fully parametrized from subthreshold measurements of impulse responses of the transient visual system. This was done and the model was tested by comparison of predictions and experimental data on flashed and sinusoidal stimuli. There is a good agreement between these two although some refinements in the model seem necessary.

2 A partial differential equation

The spatiotemporal interaction such as is found in visual processing is probably an operation performed in layers of neurons, e.g., horizontal or amacrine cells. Input and output signals are then essentially situated in the same plane, or may be separated by a small medium (a membrane). Partial differential equations are often used to describe the processing of signals within a membrane. The general form of such an equation is given by

$$\sum_{k=0}^{K}\sum_{l=0}^{L}\sum_{m=0}^{M} c_{k,l,m}\frac{\partial^k}{\partial x^k}\frac{\partial^l}{\partial y^l}\frac{\partial^m}{\partial t^m}u(x,y,t) = \sum_{k=0}^{K'}\sum_{l=0}^{L'}\sum_{m=0}^{M'} d_{k,l,m}\frac{\partial^k}{\partial x^k}\frac{\partial^l}{\partial y^l}\frac{\partial^m}{\partial t^m}v(x,y,t), \tag{1}$$

where $v(x,y,t)$ and $u(x,y,t)$ are input and output signal, respectively. With this partial differention equation (PDE) the lateral information spread within the visual system is to be described.

To be able to solve a PDE given an input signal $v(x,y,t)$ the initial and boundary conditions have to be specified. We assume that the system is causal, that the spatial extension ranges from minus to plus infinity for x and y and that excitations that have bounded amplitudes cause responses with bounded amplitudes.

Further, we assume time invariance of the system: the parameters $c_{k,l,m}$ and $d_{k,l,m}$ $(k,l,m = 0,1,2,\cdots)$ are independent of t. Also we assume a processing which is locally space invariant. These assumptions lead to constants for $c_{k,l,m}$ and $d_{k,l,m}$. Contrary to the time invariance, the space invariance of the processing in the visual system is not a very common assumption. The reason for introducing this assumption is threefold. Firstly, we will concentrate on stimuli projected in the fovea. We assume processing's independence of location to be justified within this area. Secondly, we are of the opinion that before introducing more complicated models the utility of very simple models to account for measurement data should be thoroughly explored. Thirdly, the assumption is in accordance with stack models (e.g., Koenderink and van Doorn, 1978), where in each layer homogeneous processing takes place. We assume that the transient system can be seen as a layer within such a stack model, presumably the layer with the largest receptive fields and the largest extent.

Next the PDE is assumed to be rotation-symmetrical. Although we know of physiological findings that contradict this assumption (e.g., orientation sensitivity), this restriction is imposed for the same reason as for the location-independent processing: the parsimony principle. Furthermore, there is psychophysical evidence of isotropic processing of visual stimuli by the transient system (Kelly and Burbeck, 1987). We take the lowest order of linear combinations of derivatives with respect to x and y that is rotationally symmetric: we take the Laplacian $\partial^2/\partial x^2 + \partial^2/\partial y^2$ (see Brady and Horn, 1983). In the notation (1) this means that $k + l \leq 2$, $c_{1,1,m} = 0$ and $c_{2,0,m} = c_{0,2,m}$ for the lefthand side. To ensure that the response tends to zero for stimuli with increasing spatial frequency we have to take $K' = L' = 0$.

We now have a PDE with only temporal differentiations on the right-hand side. Consequently, the right-hand side does not contribute to any spatiotemporal coupling. Therefore, an input signal $i(x, y, t)$ is introduced, which is defined by

$$i(x,y,t) = \sum_{m=0}^{M'} d_{0,0,m} \frac{\partial^m}{\partial t^m} v(x,y,t). \tag{2}$$

Replacing the right-hand side of the PDE by $i(x, y, t)$ gives no loss of generality with respect to the spatiotemporal character of the equation and is a somewhat more convenient description.

The last restriction we make on the PDE is the choice of the highest partial differentiation with respect to time. From analysis of experimentally obtained impulse responses it was found that the spatiotemporal coupling in the transient system is of a second-order temporal nature in a first-order approximation (den Brinker, 1989a; see also section 7). Therefore we take $M = 2$.

All the assumptions lead to a very simple PDE to describe the spatiotemporal coupling:

$$\sum_{m=0}^{2} \left[-A_m \left\{ \frac{\partial^2}{\partial x^2} + \frac{\partial^2}{\partial y^2} \right\} + B_m \right] \frac{\partial^m}{\partial t^m} u(x,y,t) = i(x,y,t), \tag{3}$$

$$A_m = -c_{0,2,m} = -c_{2,0,m}, \tag{4}$$

$$B_m = c_{0,0,m}. \tag{5}$$

Although this class of partial differential equations is very limited, it contains some equations that are often used in physics. It comprises, for example, the diffusion and the wave equation. A combined diffusion and wave equation takes the form

$$-\left\{ \frac{\partial^2 u}{\partial x^2} + \frac{\partial^2 u}{\partial y^2} \right\} + \frac{1}{v^2} \frac{\partial^2 u}{\partial t^2} + \frac{\beta}{v} \frac{\partial u}{\partial t} + \frac{\beta^2}{4} u = i(x,y,t), \tag{6}$$

and is within the above-mentioned class of PDEs.

3 The transfer function

We assume that only signals $i(x, y, t)$ and $u(x, y, t)$ occur for which Fourier transforms with respect to the spatial variables and a Laplace transform with respect to the time variable exist. The Fourier transform $G_F(\omega_x)$ of a function $g(x)$ is taken as

$$G_F(\omega_x) = \mathcal{F}_x\{g(x)\} = \int_{-\infty}^{\infty} g(t)\exp(-j\,\omega_x x)\,dx\,, \qquad j = \sqrt{-1}. \tag{7}$$

(The Fourier transform $G_F(\omega_y)$ of a function $g(y)$ is defined similarly.) The Laplace transform $G_L(s)$ of a causal function $g(t)$ is taken as

$$G_L(s) = \mathcal{L}_t\{g(t)\} = \int_0^{\infty} g(t)\exp(-s\,t)\,dt. \tag{8}$$

The transforms $I(\omega_x, \omega_y, s)$ and $U(\omega_x, \omega_y, s)$ of the signals $i(x, y, t)$ and $u(x, y, t)$ are defined by

$$I(\omega_x, \omega_y, s) = \mathcal{F}_x\mathcal{F}_y\mathcal{L}_t\{i(x, y, t)\}, \tag{9}$$

$$U(\omega_x, \omega_y, s) = \mathcal{F}_x\mathcal{F}_y\mathcal{L}_t\{u(x, y, t)\}. \tag{10}$$

Since in our case the spatial dimensions of the stimulus are expressed in degrees, the spatial angular frequencies ω_x and ω_y are expressed in dg^{-1}. With the help of these transforms the PDE is changed into an explicit relation between the input and output signal:

$$\sum_{m=0}^{2}\{A_m(\omega_x^2 + \omega_y^2) + B_m\}s^m\,U(\omega_x, \omega_y, s) = I(\omega_x, \omega_y, s). \tag{11}$$

The transfer function $H(\omega_x, \omega_y, s)$ is defined as the ratio of the transforms of response and excitation, so that

$$H(\omega_x, \omega_y, s) = \frac{U(\omega_x, \omega_y, s)}{I(\omega_x, \omega_y, s)} = \frac{1}{\sum_{m=0}^{2}\{A_m(\omega_x^2 + \omega_y^2) + B_m\}\,s^m}. \tag{12}$$

With the transfer function $H(\omega_x, \omega_y, s)$ is associated a function $h(x, y, t)$, by

$$H(\omega_x, \omega_y, s) = \mathcal{F}_x\mathcal{F}_y\mathcal{L}_t\{h(x, y, t)\} \tag{13}$$

The (causal) function $h(x, y, t)$ is called Green's function. Green's function gives the relation between excitation and response in the spatial and temporal domain by a convolution:

$$u(x, y, t) = h(x, y, t) * i(x, y, t), \tag{14}$$

where $*$ denotes convolution over x, y and t.

As a consequence of the assumed rotation symmetry of the processing, the transfer function $H(\omega_x, \omega_y, s)$ is not dependent on ω_x and ω_y separately, but on the sum of squares of ω_x and ω_y. The (rotation-symmetric) spatial angular frequency w is therefore introduced by

$$w = \sqrt{\omega_x^2 + \omega_y^2}, \tag{15}$$

and thus the transfer function is dependent on w and s

$$H(\omega_x, \omega_y, s) = H(w, s) = \frac{1}{\sum_{m=0}^{2}\{A_m\,w^2 + B_m\}\,s^m}. \tag{16}$$

Similarly, Green's function $h(x, y, t)$ is rotation-symmetrical, and depends on the radius $r = \sqrt{x^2 + y^2}$, so that

$$h(x, y, t) = h(r, t). \tag{17}$$

The relation between the transfer function $H(w,s)$ and Green's function $h(r,t)$ is given by a Hankel transform $\mathcal{H}_r$ and a Laplace transform:

$$H(w,s) = 2\pi\, \mathcal{H}_r \mathcal{L}_t\{h(r,t)\}, \tag{18}$$

where the Hankel transform $G_H(w)$ of a function $g(r)$ is given by

$$G_H(w) = \mathcal{H}_r\{g(r)\} = \int_0^\infty g(r)\, r\, J_0(wr)\, dr, \tag{19}$$

and where J_0 is the Bessel function of zeroth order and first kind.

From the transfer function $H(w,s)$ (eq. (16)) it can be seen that there are six free parameters: A_i and B_i for $i = 0,1,2$. Eigenfunctions of the system are Bessel functions J_0 in the spatial domain. In the temporal domain complex exponentials are the eigenfunctions. Thus, taking as input signal $i(x,y,t) = J_0(w_0\sqrt{x^2+y^2})\cos(\omega_0 t)$ gives as response the signal $u(x,y,t)$, where

$$u(x,y,t) = |H(w_0, j\omega_0)|\, J_0(w_0\sqrt{x^2+y^2})\cos(\omega_0 t + \phi), \tag{20}$$

and where

$$\phi = \arg\{H(w_0, j\omega_0)\}. \tag{21}$$

Taking as input signal $i(x,y,t) = J_0(w_0\sqrt{x^2+y^2})\,\delta(t)$ gives an output signal which is the product of the spatial modulation $J_0(w_0\sqrt{x^2+y^2})$ of the input signal and a second-order impulse response $T(t)$ in time: $u(x,y,t) = J_0(w_0\sqrt{x^2+y^2})\,T(t)$. The temporal modulation $T(t)$ is the inverse Laplace transform $\mathcal{L}^{-1}$ of the transfer function for $w = w_0$, so that

$$T(t) = \mathcal{L}^{-1}\left\{\frac{1}{\sum_{m=0}^{2}\{A_m\, w_0^2\, +\, B_m\}\, s^m}\right\}. \tag{22}$$

If the system described by (16) is to be stable, then the response of the system should be stable for arbitrary w. From (22) it is easy to see that the polynomial of s has to be a Hurwitz polynomial for each w, so the signs of the parameters A_i, B_i ($i = 0,1,2$) have to be identical. If the system is stable for arbitrary w, then the system is completely stable.

4 A membrane model

In this section an electrical network is proposed that behaves according to the class of PDEs (3) considered earlier, if adequate restrictions on its impedances are imposed (see next section). In this way, a possible realization of the class of PDEs is available and the parameters of the PDE can be interpreted and understood in a more physical representation. This realization of the PDE in the form of an electrical network has as a second advantage that it is possible to make a comparison with physiological models, since these are usually also modelled as electrical networks.

Consider a two-dimensional electrical network consisting of equal sections as shown in Figure 1. The input signal of the section at location $(m\Delta x, n\Delta y)$ is a current source $j(m\Delta x, n\Delta y, t)$, the output signal $\tilde{u}(m\Delta x, n\Delta y, t)$ is the potential at the node of the impedances. The admittance and the impedances are described as an admittance and impedances in the Laplace domain: $Y_p(s)$, $Z_1(s)$ and $Z_2(s)$. We take the admittance $Y_p(s)$ to be proportional to the area $\Delta x\Delta y$ of the section:

$$Y_p(s) = Y(s)\,\Delta x\Delta y. \tag{23}$$

$Y(s)$ is the parallel admittance of a unit area. The impedances $Z_1(s)$ and $Z_2(s)$ are taken to be proportional to the length of the sections and inversely proportional to the width, with the same proportionality factor

$$Z_1(s) = Z(s)\frac{\Delta x/2}{\Delta y}, \quad (24)$$

$$Z_2(s) = Z(s)\frac{\Delta y/2}{\Delta x}. \quad (25)$$

$Z(s)$ is the surface impedance of unit length and width. The impedance between two adjacent output signals is twice the sketched impedance, if similar sections are joined together. The current $j(m\Delta x, n\Delta y, t)$ is assumed to be proportional to the area of the section:

$$j(m\Delta x, n\Delta y, t) = \tilde{i}(m\Delta x, n\Delta y, t)\,\Delta x\,\Delta y. \quad (26)$$

The dimension of $\tilde{i}$ is the dimension of a current density.

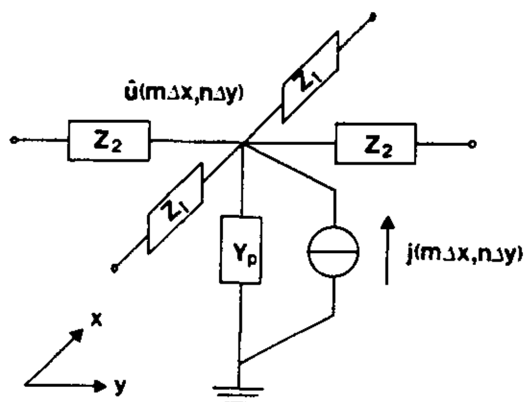

Figure 1: Section of an electrical network suggested as a model for the spatiotemporal coupling in the visual system.

Consider an infinitely large network of sections as shown in Figure 1 in both dimensions x and y. Assume furthermore that the sections Δx and Δy are infinitely small. The electrical network becomes a distributed network with a current density $\tilde{i}(x, y, t)$ as input signal and a potential $\tilde{u}(x, y, t)$ as output. Both signals are continuous distributed signals as a function of both spatial coordinates.

The transforms $\tilde{I}(\omega_x, \omega_y, s)$ and $\tilde{U}(\omega_x, \omega_y, s)$ of the signals $\tilde{i}(x, y, t)$ and $\tilde{u}(x, y, t)$ are defined by

$$\tilde{I}(\omega_x, \omega_y, s) = \mathcal{F}_x\mathcal{F}_y\mathcal{L}_t\{\tilde{i}(x, y, t)\}, \quad (27)$$

$$\tilde{U}(\omega_x, \omega_y, s) = \mathcal{F}_x\mathcal{F}_y\mathcal{L}_t\{\tilde{u}(x, y, t)\}. \quad (28)$$

The transfer function $\tilde{H}(\omega_x, \omega_y, s)$ is taken as the ratio of transforms of the input and the output signal.

$$\tilde{H}(\omega_x, \omega_y, s) = \frac{\tilde{U}(\omega_x, \omega_y, s)}{\tilde{I}(\omega_x, \omega_y, s)} = \frac{Z(s)}{(\omega_x^2 + \omega_y^2) + Z(s)Y(s)}. \quad (29)$$

From the transfer function $\tilde{H}(w,s)$ where $w = \sqrt{\omega_x^2 + \omega_y^2}$ it can be seen that
• for a stable network the ratio $Z(j\omega)Y(j\omega)$ may not be zero or negative real for any real value of ω,
• for spatiotemporal inseparable behaviour of the distributed network it is required that the ratio $Z(j\omega)Y(j\omega)$ depends on ω,
• the network is low-pass in its behaviour in the spatial angular frequency w (see Figure 2). The cut-off spatial frequency depends on the temporal angular frequency ω,
• the transfer function $\tilde{H}(w,s)$ of the distributed network of Figure 1 is the same as the transfer function $H(w,s)$ belonging to the PDE (3), if adequate restrictions are imposed on the surface impedance $Z(s)$ and the parallel admittance $Y(s)$.

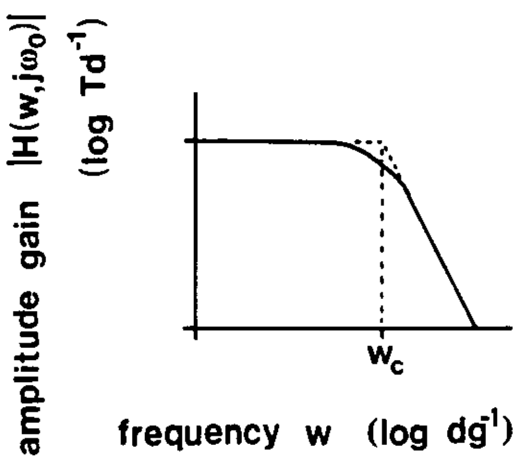

Figure 2: Amplitude characteristic $|H(w,j\omega_0)|$ as a function of the spatial frequency w. Peak value and cut-off frequency w_c of the transfer function depend on the temporal frequency ω_0. In the case that the model is used for the visual system, the units of the amplitude characteristic are in Td^{-1}.

5 The impedance and admittance of the electrical network

If the electrical network described by $\tilde{H}(w,s)$ is to be governed by the same relations between input and output signals as the class of PDEs (3) considered earlier, some restrictions have to be made on the impedance $Z(s)$ and the admittance $Y(s)$. Assume that $Y(s)$ and $Z(s)$ can be written as the ratio of two real polynomials in s, by

$$Y(s) = C_Y \frac{\prod_{i=1}^{m_Y}(s - z_{Yi})}{\prod_{i=1}^{n_Y}(s - p_{Yi})}, \tag{30}$$

$$Z(s) = C_Z \frac{\prod_{i=1}^{m_Z}(s - z_{Zi})}{\prod_{i=1}^{n_Z}(s - p_{Zi})}, \tag{31}$$

where
C_Y , C_Z amplification factors ,
z_{Yi} , z_{Zi} zeros of the admittance and the impedance, respectively ,
p_{Yi} , p_{Zi} poles of the admittance and the impedance, respectively.

We assume that all zeros z_{Yi} of the parallel admittance and all poles p_{Zi} of the surface impedance are in the left-half of the complex plane. In so far as the poles and zeros of the admittance (and of the impedance) are not real-valued, these occur in complex conjugated pairs.

Substituting (30) and (31) in the transfer function $\tilde{H}(w,s)$ (eq.29) of the electrical network the following expression for the transfer is found:

$$\tilde{H}(w,s) = \frac{C_Y \prod_{i=1}^{n_Y}(s-p_{Yi}) \prod_{i=1}^{m_Z}(s-z_{Zi})}{C_w\, w^2 \prod_{i=1}^{n_Y}(s-p_{Yi}) \prod_{i=1}^{n_Z}(s-p_{Zi}) + \prod_{i=1}^{m_Y}(s-z_{Yi}) \prod_{i=1}^{m_Z}(s-z_{Zi})}, \tag{32}$$

where $C_w = C_Y/C_Z$. Comparing $\tilde{H}(w,s)$ to $H(w,s)$ (eq.16), it is easy to see which restrictions have to be imposed on the admittance $Y(s)$ and impedance $Z(s)$ to obtain equal transfer functions for both cases. We find that

$$n_Y = m_Z = 0, \tag{33}$$

$$m_Y = n_Z = 2. \tag{34}$$

From (33) and (34) it follows that $Y(s)$ and $Z(s)$ are active elements and cannot be synthesized as impedances consisting of passive resistors, capacitors and inductances. We do not think of this as a drawback of our model, since we do not assume that neurons act as passive elements (Koch, 1984). Furthermore, if v had not been replaced by i (2) then it would be possible to realize the membrane with passive elements. However, as argued before, for our purpose it is not necessary to have zeros in the transfer function that are independent of the spatial frequency. Thus, from the point of view of simplicity, these zeros are unwanted within the membrane model.

With the restrictions (33 and 34) on the impedance and admittance the transfer function $\tilde{H}(w,s)$ can be written as

$$\tilde{H}(w,s) = \frac{C_Y}{C_w\, w^2 \prod_{i=1}^{2}(s-p_{Zi}) + \prod_{i=1}^{2}(s-z_{Yi})}, \tag{35}$$

and for equivalence of $\tilde{H}(w,s)$ and $H(w,s)$ (eq. (16)) it is found that

$$A_2 = C_Z^{-1};\quad A_1 = -2\,C_Z^{-1}(p_{Z1}+p_{Z2});\quad A_0 = C_Z^{-1}\,p_{Z1}\,p_{Z2},$$
$$B_2 = C_Y^{-1};\quad B_1 = -2\,C_Y^{-1}(z_{Y1}+z_{Y2});\quad B_0 = C_Y^{-1}\,z_{Y1}\,z_{Y2}.$$

From these equations it is seen that the parameters of the PDE (A_i, B_i, $i = 0,1,2$) can be interpreted as the zeros of a parallel admittance and the poles of the surface impedance of a distributed electrical network.

6 Root locus trajectory

It is common usage to characterize temporal behaviour by the poles of the model. Since the model considered here is a spatiotemporal one, a pole migration takes place: from (16) (and (35)) it can be seen that for each spatial angular frequency w the model acts as a second-order temporal filter. The range of (complex) values that the poles span as a function of the spatial angular frequency characterizes the model. This characteristic is a figure in the complex plane that is called the root locus diagram. As is shown in the following, the location of the poles in the complex plane forms a specific pattern, given the transfer function (16).

For any spatial frequency w the distributed network described by $\tilde{H}(w,s)$ acts as a second-order temporal filter. The temporal characteristics are described by the poles of the transfer function at w. The poles are the roots s of the quadratic characteristic equation of $\tilde{H}(w,s)$, which is given by

$$C_w\, w^2 \left\{ \prod_{i=1}^{2}(s-p_{Zi}) \right\} + \prod_{i=1}^{2}(s-z_{Yi}) = 0. \tag{36}$$

As stated before, the poles p_{Zi} (and zeros z_{Yi}), $i = 1, 2$ are both real-valued or form a complex-conjugated pair. The characteristic equation has also two real-valued or two complex-conjugated solutions.

For $w = 0$ the poles of $\tilde{H}(w, s)$ are the zeros of $Y(s)$, and for $w \to \infty$ the poles of $\tilde{H}(w, s)$ are the poles of $Z(s)$. The solutions s of the characteristic equation are a function of the spatial frequency w, and can be plotted in the s-plane similarly to what is usually done with feedback systems (Kuo, 1962). The same rules apply for the construction of a root locus trajectory in both cases.

If there are complex solutions of the characteristic equation (36), then these are located on a circle with centre on the real axis. The circles include the case of a circle with an infinitely large radius, i.e. a root locus which is (part of) a line parallel to the imaginary axis. In Figure 3 some examples of root locus trajectories of $\tilde{H}(w, s)$ are shown.

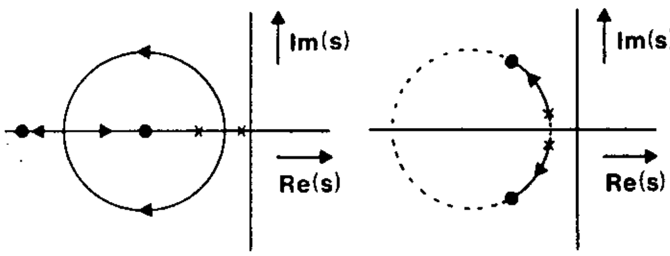

Figure 3: Two examples of root locus trajectories of $\hat{H}(w, s)$ as a function of the spatial angular frequency w. The crosses and the filled circles indicate the poles of the transfer function for $w = 0$ and $w = \infty$, respectively. The lines with the arrows indicate the direction of the pole migration with increasing w.

From psychophysical measurements it was found that larger fields (containing lower spatial frequencies) tend to temporal responses with faster oscillations. The de Lange curves have a higher peak and cut-off frequency for more extended field sizes (Granit and Harper, 1930; Roufs and Bouma, 1980; see also Section 8). Such behaviour is also found physiologically in the retina (Detwiler *et al.*, 1978, 1980).

Because of the oscillatory character of the system responses complex-valued poles are needed in the model. Furthermore, the imaginary part must increase with decreasing spatial frequency w, to account for faster responses for larger fields. Thus, contrary to cable models of nervous cells (Bennet, 1977) the surface impedances in our model cannot be taken as resistive elements. This would mean that a root locus is found with poles going to infinity for large spatial frequencies.

On similar grounds (poles going to infinity for $w \to \infty$) the combined wave and diffusion equation (6) must be rejected for a spatiotemporal model of the transient visual system. Such a PDE gives slower temporal responses for decreasing spatial frequency.

7 Parametrization of the membrane for the spatiotemporal coupling in the transient system

The question that arises is whether this spatiotemporal model can be fully parametrized from psychophysical measurements. If the model behaves similarly to the real system, we expect that by measuring the temporal behaviour of the system at several spatial frequencies the root locus of the spatiotemporal model can be found and from this the model can be parametrized, apart from a multiplication factor. Having the poles at three different spatial frequencies is sufficient to parametrize the model.

In previous studies (den Brinker and Roufs, 1989; den Brinker, 1989a) fourth-order linear filters were fitted to data from subthreshold measurements of impulse responses of circular discs with a completely dark surround (Roufs and Blommaert, 1981). These estimation procedures were also performed on data from two subjects at a 1200 Td background level for several field sizes. The results of the parameter estimations on these impulse responses are shown in Figure 4A. In this figure the estimated 90% confidence regions of the poles and zeros are plotted. From Figure 4A it can be seen that one pole pair (the one with largest norm) is shifting, if we compare the estimates obtained from the impulse responses of discs of different size. The estimate of the other pole seems to be independent of the diameter of the stimulus.

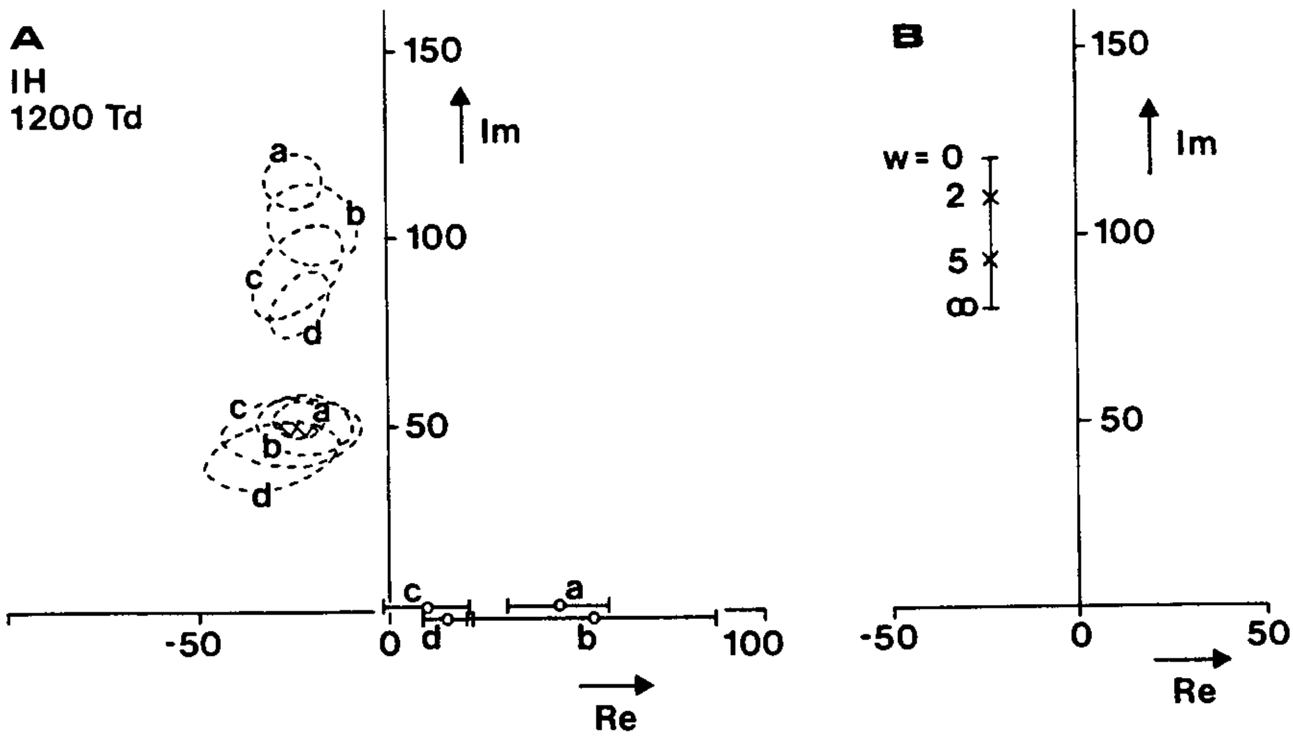

Figure 4: Pole-zero plots in the complex plane. Horizontal and vertical axis are the real and imaginary axis, respectively. The units are in s^{-1}. The lower part of the s-plane is not shown in this plot. **A** Pole-zero plot of filter parameters of a fourth-order linear filter determined from experimentally obtained impulse responses. Subject IH, 1200Td, for field diameters of 5.5 (a), 1.0 (b), 0.50 (c) and 0.28 (d) degrees. The ellipses give estimates of the 90% confidence regions of the poles. The estimated poles are located in the centres of the ellipses. The zeros are indicated by a small circle and the bars give the 90% confidence intervals. (Replot from den Brinker, 1989a.) **B** Pole-zero plot of the membrane model as a function of the spatial frequency w (see text).

An impulse response described by such a location of the poles (Fig. 4A) is shown in Figure 5 for subject IH at 1200 Td and a 30' field diameter, together with the data of the experimentally determined impulse response (see Roufs and Blommaert, 1981).

In den Brinker (1989a) it was therefore argued that the transient system could be de-

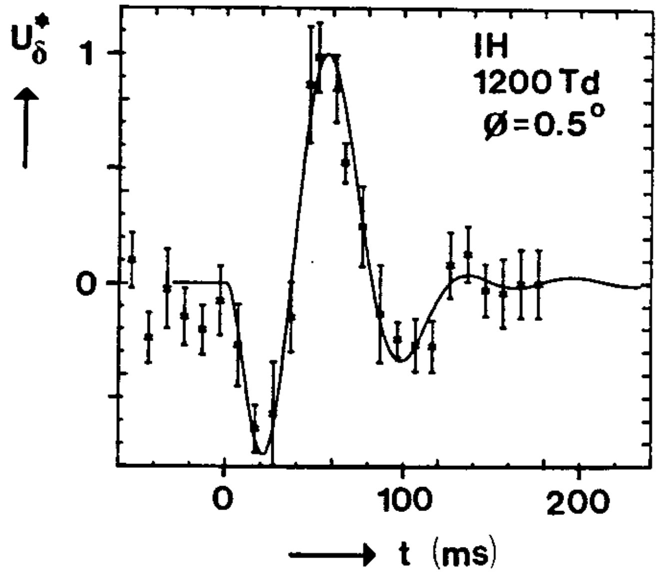

Figure 5: Experimentally determined normalized impulse response and fitted fourth-order linear filter (see den Brinker, 1989a). The bars through the experimental data points are twice the standard deviation of the mean.

scribed by two second-order filters in cascade where only one of these filters contains lateral interaction. This is shown in Figure 6, the first filter is dependent on w, the spatial frequency, the second is not. Underneath the filters are sketches of an input signal (a pulse-like stimulus), the (internal) responses from the filters L_1 and L_2, and the signal in the detection mechanism. The response of the first filter is the response of a second-order filter but the exact form depends on the field size that is used. Convolution of this second-order filter response with the impulse response of the second filter gives an impulse response shown by r_2 (Figure 6). This signal is contaminated by noise and then compared with the threshold level.

The behaviour of the largest pole as a function of the diameter of the field is reminiscent of the root locus trajectory of the membrane model (see Section 6, Figure 3). But then the plot of Figure 3 is only applicable for (zero order) Bessel functions on a background with an infinite extension, while the estimated parameters in Figure 4A are derived from discs with a completely dark surround. In the latter case the transient system is probably not operating homogeneously over space, since the lateral interaction between neurons is presumably affected by some local measure of the mean luminance.

Still, we want to make use of this kind of psychophysical data, since it so clearly demonstrates the effects of spatiotemporal coupling, and since this effect is contained in so few parameters. To be able to test the membrane model, by incorporating the data from Figure 4A, some additional assumptions about the behaviour of the model have to be made. These assumptions are:

- the parameters of the membrane model ($Y(s)$ and $Z(s)$) are locally controlled by the background,
- in the case of a sharp light-dark border the admittance $Y(s)$ seen from the light area is

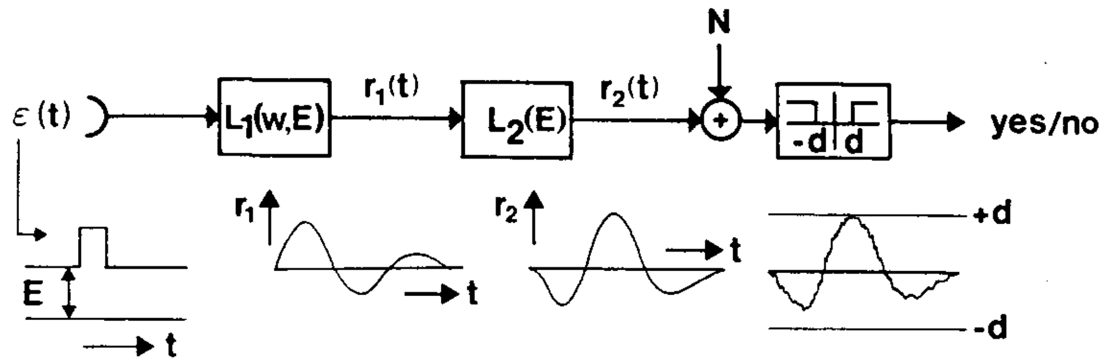

Figure 6: Spatiotemporal model of the transient visual system as suggested by den Brinker (1989a). The model consists of two linear filters, both dependent on the mean luminance E, where the first filter accounts for the spatiotemporal coupling, and the second filter is temporal only. Both filters are of a second-order temporal nature only. The last stage of the model is a detector with (symmetrical) threshold d. Underneath the sketched model a pulse-like input signal is shown, and the internal responses. The response of the first filter is a second-order filter response, where the parameters of this filter are dependent on the field diameter of the stimulus.

(virtually) infinite.
This implies that for discs of a certain diameter D, $Y(s)$ and $Z(s)$ are constant within this area, and the boundary condition for the PDE is given by $u(x,y,t) = 0$, for $(x,y) \in$ border. This, in turn, means that at a light-dark border all lateral-going signals are totally reflected (with a negative sign). The two foregoing assumptions are without doubt idealizations, but may be adequate for a first-order approximation.

The first assumption stating that the processing in the transient system adapts to the background level is trivial, except for the statement that the membrane parameters are *locally* regulated. There is physiological evidence for this assumption: horizontal cells show summation of adaptation within an area smaller than their receptive fields (Itzhaki and Perlman, 1987).

The second assumption is inspired by two perceptual findings:
- detection of temporal events upon a disc with a completely dark surround takes place at or near the centre, but never close to the border,
- if some short suprathreshold increment is given in the luminance of the disc, then a 'blob' is observed which peaks in the middle and is zero at the border.

In the case of a completely reflecting border, each rotation-symmetrical stimulus on the disc can be described as a Fourier-Bessel series (Watson, 1966), and the dynamics of the membrane within this disc area is described by the transfer function $\tilde{H}(w,s)$. For a stimulus with a diameter equal to the background, the main component in this series is the first component, which is a Bessel function J_0 (zeroth order, first kind) with spatial angular frequency

$$w = \frac{j_1}{D/2}, \tag{37}$$

where
j_1 is the first zero of this Bessel function ($J_0(j_1) = 0$),
D is the diameter of the disc.
We therefore take as a first-order approximation that for a field of diameter D, the temporal

behaviour of the membrane is dominated by the pole pair corresponding to the frequency $w = 2j_1/D$. Consequently, the largest pole in the estimated fourth-order filters of the impulse responses of discs (diameter D) with a completely dark surround is a pole that should be associated with a spatial frequency $w = 2j_1/D$.

In this way, impulse responses of discs with a completely dark surround of three different diameters (same subject and background level) can be used to parametrize the membrane model. Admittedly, this procedure to obtain parameters of the membrane from this impulse responses relies heavily upon some non-trivial assumptions. Nevertheless, we will show that this rough procedure can give some indication whether the simple membrane model presented in the foregoing can be used to describe the spatiotemporal coupling within the transient visual system.

8 Predictions from the model

Model parameters

Parameter estimations of fourth-order filters (den Brinker and Roufs, 1989; den Brinker, 1989a; see also Figure 4A) have been applied to experimentally determined impulse responses (Roufs and Blommaert,1981; Blommaert and Roufs, 1987). The membrane parameters were derived from these estimates in the manner suggested in the previous section. It was found that the parameters of the membrane are (approximately) $C_w = 0.07$, $z_{Y1}, z_{Y2} = -23 \pm j120\ \mathrm{s}^{-1}$ and $p_{Z1}, p_{Z2} = -23 \pm j70\ \mathrm{s}^{-1}$. The amplification factor C_Y was taken to be unity. The root locus diagram is shown in Figure 4B and the resemblance with the behaviour of pole with the largest norm estimated from the impulse responses can be clearly seen from comparison with Figure 4A.

The second filter L_2 (Figure 6) is a second order temporal filter with transfer function $H_2(s)$ (see den Brinker, 1989a):

$$H_2(s) = \frac{A(s-z)}{(s-p)(s-p^*)}, \tag{38}$$

where A is an amplification factor and p, p^* and z are the poles and zero of the transfer function. The parameter values of this filter were derived from the estimates performed on the impulse response over different subjects at 1200 Td and for 1° fields. These values were taken to be $p = -23 + j45\ \mathrm{s}^{-1}$, $z = 15\ \mathrm{s}^{-1}$ and $A = 0.6 \cdot 10^8$.

For both the parameters in the membrane as for the parameters of filter L_2 rounded values were taken in view of the variances in the estimates from which these parameters were derived (den Brinker, 1989a). The model presented above is totally deterministic, no effects of probability summation (either in time or over space) are taken into account.

Predictions of the model with the above mentioned parameters were made of threshold-versus-duration curves and amplitude gain characteristics for fields of different sizes with a dark surround. These predictions will be compared in the sequel with experimental data. But first the experimental apparatus and procedure are described.

Apparatus and procedure

In both the threshold-versus-duration and the de Lange measurements, the stimulus was a centrally fixated circular field of diameter 0.25, 0.5, 1.0, 2.0 or 5.0 degrees with a dark surround. The stimulus was presented (monocularly) in Maxwellian view through an artificial pupil of 2 mm. The lights were generated by linearised glow modulators, operated around a suitable working point. The luminance of the background was set by means of neutral density filters. The modulation of the background was controlled electronically by function generators. The modulation was either a rectangular pulse of variable duration or a sinusoid with variable frequency. The duration of the sinusoid was 0.8 *s* and was slowly switched on and off by a ramp function which lasted for 0.25 *s*. The amplitude of the desired function could be adjusted using a *dB* step attenuator. The calibration of the dynamic stimuli was checked before every session by means of a photomultiplier tube, properly corrected with respect to spectral sensitivity.

A P800 mini computer guided the experiments. The subject had one knob to release the stimulus, which was delayed for 300 *ms*. The beginning of the stimulus was marked by an acoustic signal. "Yes" or "No" answers were directly fed into the computer. For a certain modulation amplitude 10 identical stimuli were presented successively and the detected percentage was determined by the computer and used for generating the next modulation amplitude. In each case, the 50% threshold amplitude was determined by linear regression from at least 2 amplitude values with detection chances between 20% and 80%. This was done four times for each duration (in the threshold-versus-duration characteristic) or frequency (in the de Lange experiment). The durations and frequencies were presented in counterbalance (two sessions in counterbalance provide four estimates of the threshold amplitude).

Two subjects participated in all experiments: LT and BdB, both male and ages at the time of the experiment 36 and 30, respectively. Furthermore, subjects HD and IH (aged 28 and 43, respectively) also provided data on the normfactors. All subjects had normal acuity, although some of them used a slight correction.

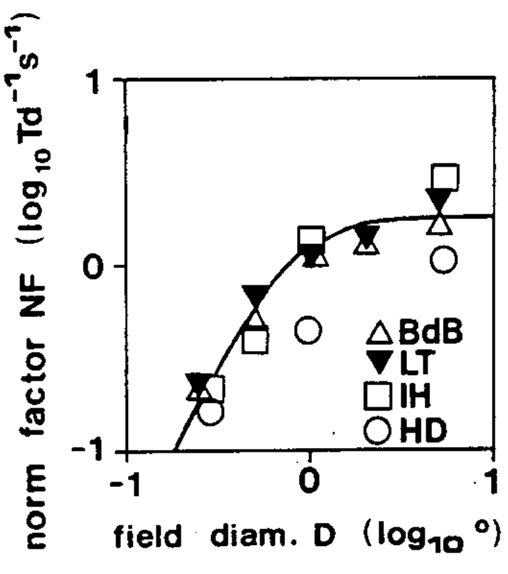

Figure 7: The norm factor of shortly flashed circular disc with a dark surround at a 1200 Td background level as a function the field diameter. The line is the prediction from the model (see text), the symbols represent the experimental data for different subjects as indicated.

Results

In the first experiment threshold-versus-duration curves were determined as a function of field size. Only a very limited number of durations was used in the measurement. Essentially, to determine the normfactor NF only one duration within Bloch's region is necessarily. The normfactor is the inverse of the energy of such pulse to reach threshold:

$$NF = 1/(\varepsilon\,\vartheta), \tag{39}$$

where
ε the amplitude of the pulse at threshold level,
ϑ the duration of the pulse.
The thresholds of several pulses with a duration outside Bloch's region were also determined to check whether the threshold-versus-duration curves had a dip at intermediate durations. This was always the case for the field sizes that were used in the experiments and is interpreted as indication that the transient system determined the response. For smaller field sizes the sustained system starts to determine the response and (of course) cannot be used as verification of the model. Also the largest field size was taken as 5° in diameter to ensure that there are no areas stimulated very far outside the fovea (see also Discussion).

In Figure 7 the normfactor NF is plotted versus the field diameter. The model predicts a slope of 2 (on log-log basis) for small diameters and a constant level for large field sizes. The experimental data agrees nicely with the prediction, although one should maybe allow a subject dependent spatial integration. (Mainly the parameter C_w in the model determines the transition point from slope 2 to a constant level). Only data from subject HD do not seem to fit the predictions; this is probably due to the fact that for this subject large gaps in time existed between the measurements of the norm factors of different field sizes.

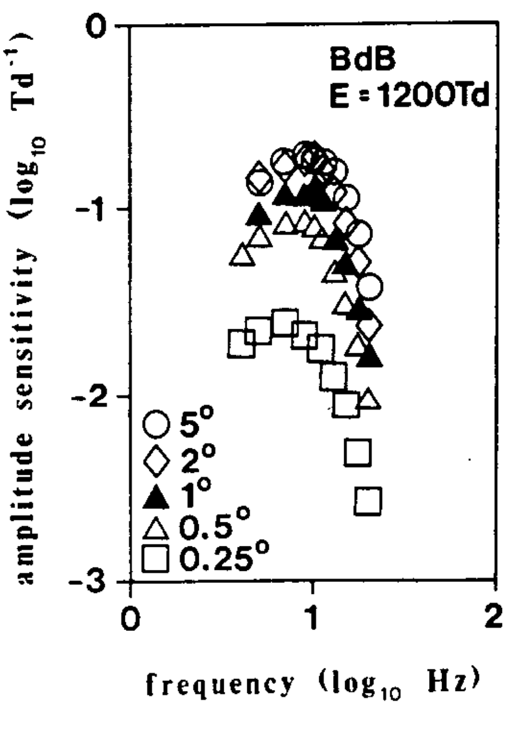

Figure 8: de Lange curves of subject BdB at 1200 Td background for different field sizes (as indicated in the figure).

In Figure 8 de Lange curves are shown (subject BdB, 1200 Td background) for several field sizes. From this figure the top value (the sensitivity factor S) and the cut-off frequency f_h

(0.3 log units below S) were taken as characteristic quantities of the high frequency side (and thus of the transient system). These data were replotted in Figure 9 as a function of field size, together with data from a second subject (LT, 1200 Td background level). The model predicts a slope 2 (on log-log basis) for the sensitivity factor of fields with a small diameter, and a constant sensitivity factor for large field sizes. The experimental data confirms this (Fig. 9A). The prediction is for all field sizes about 0.2-0.3 log units below the experimental data, an amount that can be easily attributed to probability summation over time (Roufs, 1974b; Roufs and Pellegrino, 1976). The cut-off frequency (Fig. 9B) increases both in the model simulations and in the experimental data with an increase in field size (see also Granit and Harper, 1930; Roufs and Bouma, 1980). The model predicts values for the cut-off frequency that are too high in comparison to the experimental data. Apart from the fact that it is not always easy to make a good estimate of the cut-off frequency from the experimental data, this discrepancy was already noted before. The fourth-order estimates as derived from the impulse response measurements show a fall-off in their gain that is too slow (den Brinker, 1989a) and consequently provide a too high estimate of the cut-off frequency (see also Discussion).

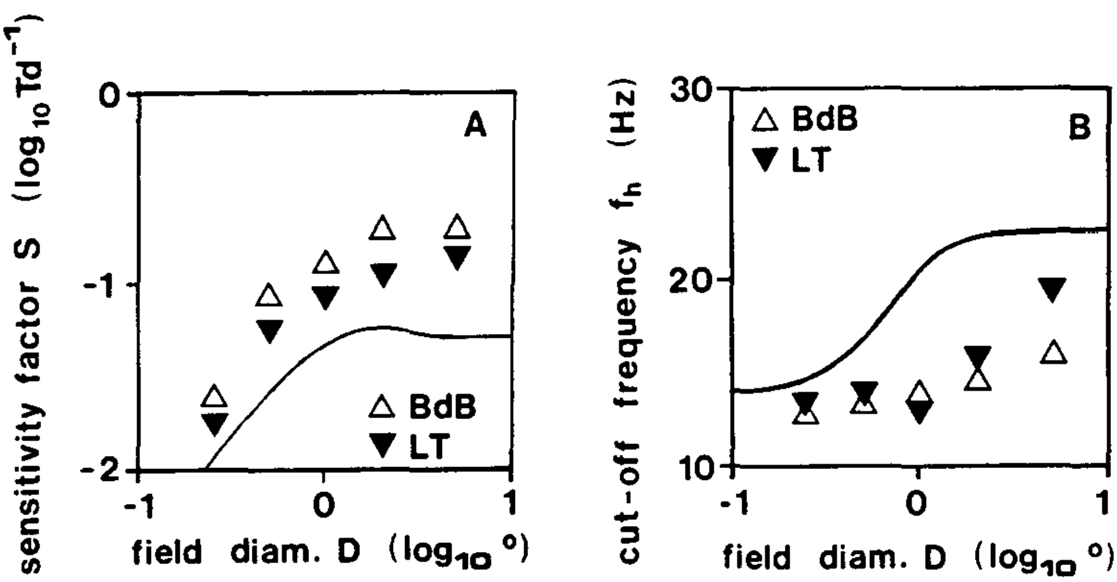

Figure 9: **A** The sensitivity factor S and **B** the cut-off frequency f_h as a function of the of the field diameter. The line represents the prediction from the model (see text), the symbols show the experimental data for two different subjects.

9 Discussion

In this article a linear model is presented as a model for spatiotemporal coupling within the transient visual system. The model is described by a PDE. This PDE is of a very simple form because of the many restrictions imposed on it (linearity, time and space invariance, rotation symmetry, low order of the PDE). The many restrictions are simultaneously the weak and strong features of the model. The strong point is the simplicity and the parsimony in parameters of the model. The weak point is the set of many major assumptions which have to be made regarding the model in order to obtain such a simple description.

The model does not agree with the current idea of local processing of visual stimuli. But then, the model presented here should account for the transient system, i.e. the channel with the largest spatial interactions. We suppose that approximation with an infinitely outstretched processing over space is a good approximation to that with a large yet finite window.

The PDE can be seen as belonging to a distributed electrical network. The system is low-pass in the spatial domain, for each temporal frequency. Alternatively, the filter is of a second-order temporal nature for each spatial frequency. The temporal behaviour of the model with variation of the spatial modulation can be seen from a root locus trajectory. The model can be fully parametrized given a proper root locus trajectory.

In den Brinker (1989a) parameter estimations of subthreshold measured impulse responses were discussed. From these kinds of psychophysical measurements the suggested spatiotemporal model can be parametrized. This results in a simple spatiotemporal model for the transient visual system as is shown in Figure 6 and consists of the membrane model in cascade with a temporal filter (of second-order) and a detection unit. The model can be completely parametrized from the estimated fourth-order linear filters of the experimentally determined impulse responses leaving no free parameters in the model.

The membrane behaviour is qualitatively similar to physiological findings in the rod network (Detwiler *et al.*, 1980). The rationale of such coupling as suggested by Detwiler *et al.* (1978, 1980) is a trade-off between the need for large spatial integration and long temporal integration in order to obtain an internal response level (for signals with small amplitude) that is large enough to exceed the internal noise level.

The membrane model was quantitatively tested by comparing predictions of normfactors, sensitivity factors and cut-off frequencies to experimental data. Making allowances for the fact that the model is deterministic, the model performed in accordance with the experimental results over a limited range of (relatively large) stimulus dimensions presented foveally. Only the cut-off frequency of the model was always found to be too high in the model. This is a consequence of the fourth-order that were used as the starting point of the parametrization of the model. An easy way to overcome this problem is to use higher order filters as a model for the impulse response (den Brinker, 1989a). In the model presented here this would mean that instead of using a second-order filter for the temporal filter L_2 a higher order temporal filter would be more adequate.

From the simulations of the model it was also found that the location of the maximum in the spatial domain varied with the dimension of the stimulus. For small field sizes ($< 1^o$) the response of the membrane is completely dominated by the first Bessel function from the series that are associated with the disc, and consequently the maximum is always located in the middle of the disc. For larger field diameters the simulations showed that the maximum occurred somewhere between the centre and the border of the disc. This is in agreement with the perceptual observation that for larger field sizes the detection occurs somewhere off-centre.

The model is open for further detailing. The responses from the membrane may be considered as rough approximations to actual occurring retinal cell responses. We did not refine the membrane responses in this way since in the first place we are interested in psychophysical modelling and, secondly, given the presented results, we do not think that such approach is very fruitful. For psychophysical modelling some refinements are needed. For instance, the predicted temporal frequency fall-off of the model is rather low (0.9 log unit per octave) in comparison with the de Lange characteristics. Furthermore, it may be worthwhile to confront the membrane model with the matched filter model we presented elsewhere (den Brinker, 1989b). The idea behind the latter model would be that response of the membrane is transmitted to the cortex, presumably a process in which a large amount of noise is introduced. If cortical cells act in such a way as to minimize these noise influences and if the system acts linearly around threshold level (de Lange,1952; Krauskopf, 1980; Roufs and Blommaert, 1981; Blommaert and Roufs, 1987), then the temporal filter should have the characteristics of a matched filter (den Brinker, 1989b). In this way not only an appropriate fall-off of the gain characteristic can be obtained and presumably a better prediction of the cut-off frequency, but simultaneously this would provide a functional interpretation of the filter L_2 (see Figure 6).

Another possibility for further research lies in extending the membrane properties to extra-foveal phenomena by introducing slowly varying admittance and impedance values ($Y(s)$, $Z(s)$) as a function of eccentricity. Also, the behaviour of these parameters with background level may yield interesting interpretations. In this way maybe phenomena as found by Rovamo and Raninen (1984) and Raninen and Rovamo (1986) can be accounted for within the model.

Acknowledgements

The author is grateful to Prof. J.A.J. Roufs and J.B. Martens for their advice on an early version of the manuscript. Thanks to P. Theelen for his help and advice in the experiments.

References

Bennet, M.V.L. (1977) Electrical transmission: a functional analysis and comparison to chemical transmission. In: *Handbook of Physiology*. Bethesda Md: American Physiological Society.

Blommaert, F.J.J. and J.A.J. Roufs (1987) Prediction of thresholds and latency on the basis of experimentally determined impulse responses. Biol. Cybern. **56**, 329-344.

Brady, M. and B.K.P. Horn (1983) Rotationally symmetric operators for surface interpolation. Computer Vision, Graphics, and Image Processing **22**, 70-94.

Breitmeyer, B.G. and L. Ganz (1976) Implications of sustained and transient channels for theories of visual pattern masking, saccadic suppression, and information processing. Psychol. Review **83**, 1-36.

Brinker, A.C. den (1989a) A comparison of results from parameter estimations of impulse responses of the transient visual system. Biol. Cybern **61**, 139-151.

Brinker, A.C. den (1989b) *Modelling the transient visual system.* Dr. Thesis Eindhoven Univ. of Technol.

Brinker, A.C. den and J.A.J. Roufs (1989) Nonlinear parameter estimation applied to psychophysically measured impulse responses. IEEE Trans. Biomed. Eng. **36**, 346-354.

Cleland, B.G., M.W. Dubin and W.R. Levick (1971) Sustained and transient neurones in the cat's retina and lateral geniculate nucleus. J. Physiol. **217**, 473-496.

Detwiler, P.B., A.L. Hodgkin and P.A. McNaughton (1978) A surprising property of electrical spread in the network of rods in the turtle's retina. Nature **274**, 562-565.

Detwiler, P.B., A.L. Hodgkin and P.A. McNaughton (1980) Temporal and spatial characteristics of the voltage response of rods in the retina of the snapping turtle. J. Physiol. **300**, 213-250.

Granit, R. and P. Harper (1930) Comparative studies on the peripheral and central retina. II. Synaptic reactions in the eye. Am. J. Physiol. **95**, 211-228.

Itzhaki, A. and I. Perlman (1987) Light adaptation of red cones and L1-horizontal cells in the turtle retina: effect of the background spatial pattern. Vision Res. **27**, 685-696.

Kelly, D.H. and C.A. Burbeck (1987) Further evidence for a broadband, isotropic mechanism sensitive to high-velocity stimuli. Vision Res. **27**, 1527-1537.

Koch, C. (1984) Cable theory in neurons with active, linearized membranes. Biol. Cybern. **50**, 15-33.

Koenderink, J.J. and A.J. van Doorn (1978) Visual detection of spatial contrast; influence of location in the visual field, target extent and illuminance level. Biol. Cybern. **30**, 157-167.

Korn, A. and W. von Seelen (1972) Dynamische Eigenschaften von Nervennetzen im visuellen System. Kybernetik **10**, 64-77.

Krauskopf, J. (1980) Discrimination and detection of changes in luminance. Vision Res. **20**, 671-677.

Kulikowski, J.J. and D.J. Tolhurst (1973) Psychophysical evidence for sustained and transient detectors in human vision. J. Physiol. **232**, 149-162.

Kuo, B.C. (1962) *Automatic Control Systems.* Englewood Cliff N.J.: Prentice-Hall.

Lange, H. de (1952) Experiments on flicker and some calculations on an electrical analogue of the foveal system. Physica **18**, 935-950.

Legge, G.E. (1978) Sustained and transient mechanisms in human vision: temporal and spatial properties. Vision Res. **18**, 69-81.

Mandler, M.B. and W. Makous (1984) A three-channel model of temporal frequency perception. Vision Res. **24**, 1881-1887.

Marko, H. (1981) The z-model - a proposal for spatial and temporal modeling of visual threshold perception. Biol. Cybern. **39**, 111-123.

Raninen, A. and J. Rovamo (1986) Perimetry of critical flicker frequency in human rod and cone vision. Vision Res. **26**, 1249-1255.

Roufs, J.A.J. (1974a) Dynamic properties of vision-IV. Thresholds of decremental flashes, incremental flashes and doublets in relation to flicker fushion. Vision Res. **14**, 831-851.

Roufs, J.A.J. (1974b) Dynamic properties of vision-VI. Stochastic threshold fluctuations and their effect on flash-to-flicker sensitivity ratio. Vision Res. **14**, 871-888.

Roufs, J.A.J. and F.J.J. Blommaert (1981) Temporal impulse and step responses of the human eye obtained psychophysically by means of a drift-correcting perturbation technique. Vision Res. **21**, 1203-1221.

Roufs, J.A.J. and H. Bouma (1980) Towards linking perception research and image quality. Proc. Soc. Inf. Displ. Eng. **21**, 247-270.

Roufs, J.A.J. and J.A. Pellegrino van Stuyvenberg (1976) Gain curve of the eye to subliminal sinusoidal modulation of light. IPO Annual Progress Report **11**, 56-63.

Rovamo, J. and A. Raninen (1984) Critical flicker frequency and M-scaling of stimulus size and retinal illuminance. Vision Res. **24**, 1127-1131.

Watson, G.N. (1966) *A treatise on the theory of Bessel functions.* Cambridge: University Press.

Wilson, H.R. and J.R. Bergen (1979) A four-mechanism model for threshold spatial vision. Vision Res. **19**, 19-32.

ISSN 0167-9708
Coden: TEUEDE

(222) Jóźwiak, L.
THE FULL-DECOMPOSITION OF SEQUENTIAL MACHINES WITH THE SEPARATE REALIZATION OF THE NEXT-STATE AND OUTPUT FUNCTIONS.
EUT Report 89-E-222. 1989. ISBN 90-6144-222-2

(223) Jóźwiak, L.
THE BIT FULL-DECOMPOSITION OF SEQUENTIAL MACHINES.
EUT Report 89-E-223. 1989. ISBN 90-6144-223-0

(224) Book of abstracts of the first Benelux-Japan Workshop on Information and Communication Theory, Eindhoven, The Netherlands, 3-5 September 1989.
Ed. by Han Vinck.
EUT Report 89-E-224. 1989. ISBN 90-6144-224-9

(225) Hoeijmakers, M.J.
A POSSIBILITY TO INCORPORATE SATURATION IN THE SIMPLE, GLOBAL MODEL OF A SYNCHRONOUS MACHINE WITH RECTIFIER.
EUT Report 89-E-225. 1989. ISBN 90-6144-225-7

(226) Dahiya, R.P. and E.M. van Veldhuizen, W.R. Rutgers, L.H.Th. Rietjens
EXPERIMENTS ON INITIAL BEHAVIOUR OF CORONA GENERATED WITH ELECTRICAL PULSES SUPERIMPOSED ON DC BIAS.
EUT Report 89-E-226. 1989. ISBN 90-6144-226-5

(227) Bastings, R.H.A.
TOWARD THE DEVELOPMENT OF AN INTELLIGENT ALARM SYSTEM IN ANESTHESIA.
EUT Report 89-E-227. 1989. ISBN 90-6144-227-3

(228) Hekker, J.J.
COMPUTER ANIMATED GRAPHICS AS A TEACHING TOOL FOR THE ANESTHESIA MACHINE SIMULATOR.
EUT Report 89-E-228. 1989. ISBN 90-6144-228-1

(229) Oostrom, J.H.M. van
INTELLIGENT ALARMS IN ANESTHESIA: An implementation.
EUT Report 89-E-229. 1989. ISBN 90-6144-229-X

(230) Winter, M.R.M.
DESIGN OF A UNIVERSAL PROTOCOL SUBSYSTEM ARCHITECTURE: Specification of functions and services.
EUT Report 89-E-230. 1989. ISBN 90-6144-230-3

(231) Schemmann, M.F.C. and H.C. Heyker, J.J.M. Kwaspen, Th.G. van de Roer
MOUNTING AND DC TO 18 GHz CHARACTERISATION OF DOUBLE BARRIER RESONANT TUNNELING DEVICES.
EUT Report 89-E-231. 1989. ISBN 90-6144-231-1

(232) Sarma, A.D. and M.H.A.J. Herben
DATA ACQUISITION AND SIGNAL PROCESSING/ANALYSIS OF SCINTILLATION EVENTS FOR THE OLYMPUS PROPAGATION EXPERIMENT.
EUT Report 89-E-232. 1989. ISBN 90-6144-232-X

(233) Nederstigt, J.A.
DESIGN AND IMPLEMENTATION OF A SECOND PROTOTYPE OF THE INTELLIGENT ALARM SYSTEM IN ANESTHESIA.
EUT Report 90-E-233. 1990. ISBN 90-6144-233-8

(234) Philippens, E.H.J.
DESIGNING DEBUGGING TOOLS FOR SIMPLEXYS EXPERT SYSTEMS.
EUT Report 90-E-234. 1990. ISBN 90-6144-234-6

(235) Heffels, J.J.M.
A PATIENT SIMULATOR FOR ANESTHESIA TRAINING: A mechanical lung model and a physiological software model.
EUT Report 90-E-235. 1990. ISBN 90-6144-235-4

(236) Lammers, J.O.
KNOWLEDGE BASED ADAPTIVE BLOOD PRESSURE CONTROL: A Simplexys expert system application.
EUT Report 90-E-236. 1990. ISBN 90-6144-236-2

(237) Ren Qingchang
PREDICTION ERROR METHOD FOR IDENTIFICATION OF A HEAT EXCHANGER.
EUT Report 90-E-237. 1990. ISBN 90-6144-237-0

ISSN 0167-9708
Coden: TEUEDE

(238) Lammers, J.O.
THE USE OF PETRI NET THEORY FOR SIMPLEXYS EXPERT SYSTEMS PROTOCOL CHECKING.
EUT Report 90-E-238. 1990. ISBN 90-6144-238-9

(239) Wang, X.
PRELIMINARY INVESTIGATIONS ON TACTILE PERCEPTION OF GRAPHICAL PATTERNS.
EUT Report 90-E-239. 1990. ISBN 90-6144-239-7

(240) Lutgens, J.M.A.
KNOWLEDGE BASE CORRECTNESS CHECKING FOR SIMPLEXYS EXPERT SYSTEMS.
EUT Eeport 90-E-240. 1990. ISBN 90-6144-240-0

(241) Brinker, A.C. den
A MEMBRANE MODEL FOR SPATIOTEMPORAL COUPLING.
EUT Report 90-E-241. 1990. ISBN 90-6144-241-9